Title

The Matrix Metalloproteinase-13 Inhibitor Poricoic Acid ZI Ameliorates Renal Fibrosis by Mitigating Epithelial-Mesenchymal Transition

Journal

Molecular Nutrition & Food Research, 63(13)

ISSN

1613-4125

Authors

Chen, Lin
Cao, Gang
Wang, Ming
et al.

Publication Date

2019-07-01

DOI

10.1002/mnfr.201900132

Peer reviewed

Molecular Nutrition & Food Research
www.mnf-journal.com

The Matrix Metalloproteinase-13 Inhibitor Poricoic Acid ZI Ameliorates Renal Fibrosis by Mitigating Epithelial-Mesenchymal Transition

*Lin Chen, Gang Cao, Ming Wang, Ya-Long Feng, Dan-Qian Chen, Nosratola D. Vaziri, Shougang Zhuang, and Ying-Yong Zhao**

Scope: Fibrosis plays a key role in the progression of various diseases. Matrix metalloproteinases (MMPs) are important for epithelial-mesenchymal transition (EMT), which contributes to organ fibrosis. Four new poricoic acids are identified, poricoic acid ZI, ZJ, ZK, and ZL, as novel MMP inhibitors from edible mushroom *Poria cocos*.

Methods: Molecular docking, siRNA techniques, TGF-β1-treated renal cells, and unilateral ureteral obstructed (UUO) mice are used to explore the potential efficacy of the novel MMP inhibitors in mitigating the fibrotic process.

Results: Treatment with four poricoic acids downregulates profibrotic protein expression in TGF-β1-induced HK-2 cells. Similar results are observed in NRK-52E and NRK-49F cells, indicating that poricoic acids can suppress EMT. Furthermore, both in vitro and in vivo experiments demonstrate that poricoic acid ZI (PZI) exerts a stronger inhibitory effect on protein expression and enzymatic activity of MMP-13 than the other three compounds, which is consistent with the docking results. The inhibitory effect of PZI on MMP-13 is partially attenuated by MMP-13 RNAi in HK-2 cells and UUO mice.

Conclusions: The findings indicate that as a specific MMP-13 inhibitor, PZI attenuates EMT and renal fibrosis. Therefore, the MMP-13 inhibitor PZI can be a novel therapeutic candidate for limiting EMT and renal fibrosis.

1. Introduction

Natural products are a major source for the discovery of safe and effective medications.[1,2] Due to their relative safety and favorable therapeutic effects, natural products have drawn considerable attention for the discovery of promising compounds and drugs.[3–5] Fibrosis is an end-stage pathological feature of numerous chronic diseases that affects various organs in the body such as heart, liver, lung, and kidney.[6–8] Epithelial-mesenchymal transition (EMT) plays a central role in progressive fibrosis. Mounting evidence indicates that EMT is regulated by numerous extrinsic factors and intracellular signalling pathways such as the renin-angiotensin system (RAS), inflammation, oxidative stress, TGF-β/Smad signalling, Wnt/β-catenin signalling, lipid metabolism, gut microbiome, and microRNAs.[9–19] Although a number of drugs have been widely used to protect against fibrosis, the available strategies that specifically target the pathogenesis of fibrosis are quite limited. In a recent review, we described the efficacy of certain natural products as antifibrosis agents.[20] Many natural products have been widely applied as alternative therapeutic agents for targeting the EMT process,[21–24] which includes epithelial detachment, de novo α-SMA expression and actin reorganization, tubular basement membrane disruption, and increased cell migration and invasion. Matrix metalloproteinases (MMPs), which belong to a family of zinc-dependent endopeptidases, were originally considered to exert their antifibrotic effects through digestion of excessive matrix. Therefore, due to their ability to regulate tissue turnover during fibrogenesis, MMPs,

L. Chen, M. Wang, Y.-L. Feng, D.-Q. Chen, Y.-Y. Zhao
School of Pharmacy
Faculty of Life Science & Medicine
Northwest University
No. 229 Taibai North Road, Xi'an, Shaanxi 710069, China
E-mail: zyy@nwu.edu.cn

N. D. Vaziri
Division of Nephrology and Hypertension
School of Medicine
University of California Irvine
Irvine, CA 92897, USA

G. Cao
School of Pharmacy
Zhejiang Chinese Medical University
No. 548 Binwen Road, Hangzhou, Zhejiang 310053, China

S. Zhuang
Department of Nephrology
Shanghai East Hospital
Tongji University School of Medicine
No. 150 Jimo Road, Shanghai 200120, China

DOI: 10.1002/mnfr.201900132

including MMP-2, MMP-7, MMP-9, and MMP-13, are considered effective therapeutic targets for controlling fibrosis.

Poria cocos (Schw.) Wolf (Poliporaceae) is a well-known edible and medicinal mushroom. The sclerotia of *P. cocos*, also known as "tuckahoes" or "Indian bread,"[25] exhibits various biological activities such as antitumor, anti-inflammatory, antioxidant, and lipid-lowering effects.[26–28] Our previous studies demonstrated that the surface layer of *P. cocos* enhanced diuresis and was highly effective in the treatment of chronic kidney disease and hyperlipidaemia.[29–33] In the present study, we conducted molecular docking experiments (using AutoDock) to explore the interactions of poricoic acid ligands with MMP proteins. In addition, using in vitro experiments, we explored the inhibitory effect of the four novel poricoic acids on MMPs and the fibrotic process in cultured human and rat proximal tubular epithelial cells (HK-2 and NRK-52E, respectively), rat fibroblasts (NRK-49F), and mice with unilateral ureteral obstruction (UUO).

2. Experimental Section

2.1. Materials

All materials, reagents, solvents, and instruments were described in our previous publications.[34] All the primary antibodies and secondary antibodies were described in our previous study.[35]

2.2. Extraction and Isolation of Eleven Poricoic Acids

Four new compounds, poricoic acid ZI (PZI), poricoic acid ZJ (PZJ), poricoic acid ZK (PZK), and poricoic acid ZL (PZL), as well as seven known compounds including poricoic acid ZD (PZD), poricoic acid G (PG), poricoic acid B (PB), poricoic acid DM (PDM), poricoic acid ZC (PZC), poricoic acid AM (PAM), and poricoic acid C (PC) were isolated from the surface layer of Poria cocos by using chromatographic methods. The isolation methods of the new compounds are described in Supporting Information.

2.3. Dosage Information

All animal care and experimental procedures were approved by the Ethics Committee for Animal Experiments of the Northwest University (No. SYXK2010-004). Male BALB/c mice (6–8-week-old and weighing 18–22 g) were purchased from the Animal Center of Xi'an Jiaotong University, Xi'an, Shaanxi. Mice were provided food and water ad libitum and housed in 40–70% humidity at 22 ± 2 °C and in a 12-h light/12-h dark cycle. UUO was established based on our own previously published methods.[35] Mice were randomly divided into three groups ($n = 8$): sham, UUO, and UUO+PZI groups. The mice in the treatment groups were administered PZI (10 mg kg^{-1} per day) by gastric gavage for 7 days. Wulingsan was composed of five traditional herbal medicines, *P. cocos* Wolf, *Alisma orientale* (Sam.) Juzep, *Polyporus umbellatus* (Pers.) Fries, *Atractylodes macrocephala* Koidez, and *Cinnamomum Cassia* Presl. Our latest study demonstrated that Wulingsan treatment in patients with chronic kidney disease were significantly protected against renal fibrosis.[36] It was already indicated that daily intake of *P. cocos* at a dose of 15 g per person ameliorated renal injury in patients. The amount of PZI in *P. cocos* (15 g per day per person) from Wulingsan was equivalent to the amount mice received by oral administration. The dose of PZI was also determined based on dose-response experiments in our previous study.[35] Under general anaesthesia, the animals were sacrificed at day 7 after UUO.

2.4. Knockdown of MMP-13 in UUO Mice

Lentivirus carrying shRNA against MMP-13 and lentivirus containing nonspecific shRNA (scramble) were employed. After anaesthesia and surgery, mice were laparotomized and injected with recombinant adenovirus vector. Then, 100 μL of saline or lentivirus cocktail (1×105 IU μL^{-1}) was injected into kidney.

2.5. Molecular Docking

Molecular docking was performed using AutoDock 4.0 according to the standard procedures, and crystal structures were obtained from the RSCB Protein Data Bank (MMP-2, MMP-7, MMP-9, and MMP-13 [entry: 2y6c, 1gkc and 3o2x, respectively]). Briefly, the crystallographic ligand and water were extracted from the complex, except for zinc ion, and hydrogen atoms were added. The minimization of all compounds was carried out with MOE before docking analysis. In all dockings, the grid boxes of MMP-7, MMP-9, and MMP-13 were set at $40 \times 76 \times 42$ points, $36 \times 58 \times 74$ points, and $68 \times 68 \times 64$ points, respectively. The grid maps were centered on the ligand binding sites, and a grid spacing of 0.375 Å was used. Fifty runs were generated with the Lamarckian genetic algorithm search. The docked conformation of each compound was ranked into clusters based on the binding energy, and the top-ranked conformations were visually analyzed. Then, the position with the lowest binding energy was selected as the most suitable conformation to further analyze the interactions between compounds and proteins by using Discovery Studio 4.5.

2.6. Histological Analysis

The tissues were fixed in 4% formaldehyde and embedded by using paraffin. Kidney tissue sections (5 μm) were obtained for histological analysis. Hematoxylin-eosin (H&E) and Masson's trichrome staining was performed according to standard staining protocols.[37] Immunohistochemical staining was performed as described in a previous study.[38] All histological data were obtained in a blinded manner by two independent pathologists.

2.7. Cell Culture and Treatment

HK-2, NRK-52E, and NRK-49F cells were used to investigate the inhibitory effects of poricoic acids on TGF-β1 stimulation. Cells were cultured and treated based on our reported methods.[35,39]

The concentration of 10 μM of PZI, PZJ, PZK, and PZL was used in this study.

2.8. Cell Viability Analysis by CCK-8

The 1×10^4 cells cultured in 96-well plates were treated with different concentrations of PZI, PZJ, PZK, and PZL (0, 1, 10, 50, 100 μM) for 24 h. Cell viability analysis was performed based on our reported method.[39]

2.9. Western Blot Analysis

Cells were lysed by using RIPA lysis buffer. Western blot analysis was performed based on our previous study.[35] The relative intensity of each protein was calculated by densitometry using ImageJ software, and band density was normalized by using expression levels of α-tubulin or GAPDH.

2.10. Immunofluorescence Staining

HK-2 cells were cultured on coverslips and treated as indicated. The detailed methods are described in our previous publication.[39]

2.11. Knockdown of MMP-13 by Small Interfering RNA (siRNA)

After grown to 60% confluence, HK-2 cells were transfected with 3 μL of 10 μM MMP-13 or control siRNA in each well according to the manufacturer's protocols. Lipofectamine RNAiMAX (Invitrogen, New York, USA) was employed. Transfected cells were analyzed by Western blot.

2.12. MMP-13 Activity Assay

MMP-13 activity was determined by using SensoLyte Plus 520 specific MMP-13 assay (AnaSpec, San Jose, USA) according to the manufacturer's protocol. Detection was then carried out using a microplate reader with a filter set for excitation/emission wavelengths of 490 nm/520 nm (Thermo, New York, USA).

2.13. Statistical Analysis

The number of replicates was 6 per group for each data set, and results were presented as the mean ± SEM. Statistical analysis was performed with GraphPad Prism 5.0 software (GraphPad software, San Diego, USA). An unpaired Student's *t*-test was used for determining the significant difference between two groups. One-way ANOVA, followed by Dunnett's post hoc test, was used for analyzing the differences between various experimental variables when there were more than two groups. *p*-values <0.05 indicated statistical significance.

3. Results

3.1. Identification of the Structures of the Four New Poricoic Acids

Compound 1 was obtained as a primrose yellow amorphous powder and its molecular formula is $C_{30}H_{44}O_6$ based on the molecular ion peak[40] at m/z 499.3083 (calcd. for 499.3060) in the HRESIMS. The ^{1}H NMR spectrum (Table S1, Supporting Information) of compound 1 indicated the presence of two oxymethine hydrogens at δ_H 4.64 (m, 1H) and 4.60 (m, 1H) and two olefinic methylenes at δ_H 5.90 (s, 1H) and 5.42 (d, $J = 6.2$ Hz, 1H). The ^{13}C NMR and distortionless enhancement by polarization transfer (DEPT) spectra showed 30 carbon signals assigned to seven methyls, six methylenes, eight methines, and nine quaternary carbons. The carbon signal indicated the presence of two carbonyl groups (δc 217.4 and 214.1), one carboxyl carbon (δc 178.8), four olefinic carbons (δc 143.9, 141.3, 128.4, and 119.7), and two oxymethine carbons (δ_C 76.4 and 67.6). Detailed examination by analysis of ^{1}H-detected heteronuclear single quantum coherence spectrum (HSQC) completed the establishment of connection between the ^{1}H protons to their directly connected ^{13}C signals. The heteronuclear multiple bond coherence spectroscopy (HMBC) correlations of δ_H 1.03 (H-26) and 1.04 (H-27) with δ_C 214.1 (C-24) confirmed the presence of carbonyl at C-24. The correlations of δ_H 4.64 (H-6) with δ_C 128.4 (C-7) and δ_C 141.3 (C-8) indicated that the hydroxyl group was located at C-6, which was confirmed by ^{1}H-^{1}H shift correlation spectroscopy (^{1}H-^{1}H COSY) correlating δ_H 4.64 (H-6) with δ_H 2.85 (H-5) and δ_H 4.64 (H-6) with δ_H 5.90 (H-7). The orientation of the hydroxyl group at C-6 was assigned as β-orientation based on the nuclear overhauser effect spectroscopy (NOESY) correlation between H-6 and H-5. Therefore, compound 1 was identified as (20R)-6β,16α-dihydroxy-3,24-dioxo-lanosta-7,9(11)-diene-21-oic acid, named PZI.

Compound 2 was obtained as a white amorphous powder and had a molecular formula of $C_{31}H_{48}O_5$ based on the molecular ion peak $[M+Na]^+$ at m/z M = 523.3398 (calcd. for 523.3399) in the HRESIMS. The ^{1}H NMR spectrum (Table S1, Supporting Information) of compound 2 indicated the presence of one oxymethine hydrogen at δ_H 4.19 (dd, $J = 9.7$, 5.7 Hz, 1H) and two olefinic methylenes at δ_H 4.92 (d, $J = 1.5$ Hz, 1H), 4.76 (s, 1H), 4.71 (s, 1H), and 4.68 (d, $J = 1.1$ Hz, 1H). The ^{13}C NMR and the DEPT spectra showed 31 carbon signals assigned to six methyls, eleven methylenes, five methines, and nine quaternary carbons. The carbon signal indicated the presence of two carboxyl carbons (δc 180.6 and 178.5), two olefinic carbons (δc 140.3 and 131.3), and one oxymethine carbon at δ_C 73.8. The^{1}H-^{1}H COSY correlations of H-15 (δ_H 4.19) with H-16 (δ_H 1.95 and 1.81) and the correlation between H-15 (δ_H 4.19),C-17 (δ_H 47.2) and C-30 (δ_C 18.9) in the HMBC experiment (**Figure 1**) indicated that the hydroxyl group was connected to C-15. The NOESY cross peaks of H-15/H-18 and H-15/H-20 suggested the α-orientation assignment of OH-15 (Figure 1). Therefore, compound 2 was identified as (20R)-15α-hydroxy-3,4-seco-lanosta-4(28),8(9),24(31)-triene-3,21-dioic acid, named PZJ.

Compound 3 was obtained as a white amorphous powder and had a molecular formula of $C_{31}H_{48}O_4$ based on the molecular ion peak $[M+Na]^+$ at m/z 507.3435 (calcd. for 507.3450)

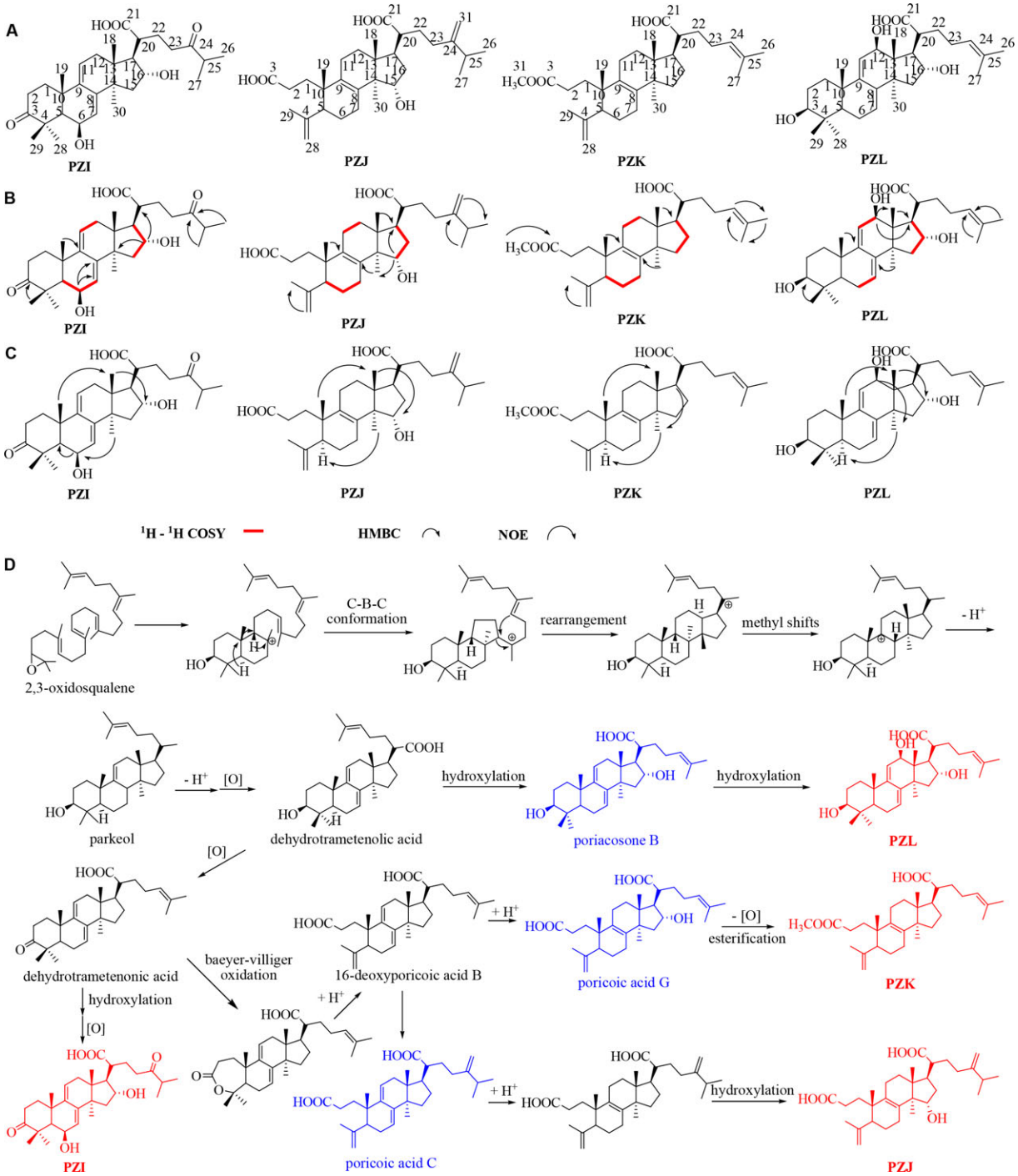

Figure 1. Four novel lanostane triterpenoids and the hypothetical biosynthetic pathways of poricoic acids. A) Chemical structures of compounds PZI, PZJ, PZK, and PZL. B) Key HMBC correlations (from H to C) and ^{1}H-^{1}H COSY correlations of PZI, PZJ, PZK, and PZL. C) Key NOESY correlations of PZI, PZJ, PZK, and PZL. D) Hypothetical biosynthetic pathways of PZI, PZJ, PZK, and PZL and known triterpenoids originating from 2,3-oxidosqualene.

in the HRESIMS. The ^{1}H NMR data (Table S1, Supporting Information) showed seven methyls at δ_H 3.66 (s, 3H), 1.77 (s, 3H), 1.69 (s, 3H), 1.61 (s, 3H), 0.96 (s, 6H), and 0.81 (s, 3H), and three olefinic protons at δ_H 4.69 (s, 1H), 4.92 (s, 1H), and 5.11 (t, J = 7.0 Hz, 1H). The ^{13}C NMR and DEPT spectra (Table S1, Supporting Information) showed 31 carbon signals assigned to seven methyls, eleven methylenes, four methines, and nine quaternary carbons. The NMR spectroscopic data of compound 3 were similar to those of poricoic acid G,[26] except the resonances for CH-16 (δ_H/δ_C 4.52/76.7) were exchanged by CH_2-16 (δ_H/δ_C 1.36/27.1) and the presence of the methoxy group (δ_H/δ_C 3.66/51.7), indicating a dehydroxylation at C-16 and an

esterification at C-3. This was also verified by the correlation of CH_3-31 (δ_H 3.66) with C-3 (δ_C 175.0) in the HMBC spectra (Figure 1). Therefore, compound 3 was identified as (20R)-3,4-seco-lanosta-4(28),8(9),24(25)-triene-21-oic acid 3-oate, named PZK.

Compound 4 was obtained as a white amorphous powder and had a molecular formula of $C_{30}H_{46}O_5$ based on the molecular ion peak $[M+H]^+$ at m/z 487.3340 (calcd. for 487.3424) in the HRESIMS. The ^{1}H NMR spectrum (Table S1, Supporting Information) of compound 4 indicated the presence of three oxymethine hydrogens at δ_H 4.90 (s, 1H), 4.62 (s, 1H), and 3.44 (s, 1H) and three olefinic methylenes at δ_H 5.62 (s, 1H), 5.59 (s, 1H), and 5.34 (s, 1H). The ^{13}C NMR and DEPT spectra showed 30 carbon signals assigned to seven methyls, six methylenes, nine methines, and eight quaternary carbons. The carbon signal indicated the presence of one carboxyl carbon (δc 180.8) and three oxymethine carbons (δ_C 78.2, 75.4 and 73.9). In the HMBC experiment, there were correlations of H-12 (δ_H 4.90) with C-17 (δ_C 57.8) and C-18 (δ_C 23.2). Combined analysis of^{13}C NMR and DEPT data of the 12 carbon atoms (δ_C 73.9) showed that the hydroxyl group was connected to C-12. This was verified by the correlation between H-12 (δ_H 4.90) and H-11 (δ_H 5.62) in the ^{1}H-^{1}H COSY spectra. The NOESY cross peaks of H-12/H-30 suggested the β-orientation assignment of OH-12 (Figure 1). Therefore, compound 4 was identified as (20R)-3β,12β,16α-trihydroxy-lanosta-7,9(11),24(25)-triene-21-oic acid, named PZL.

In addition, the structures of known compounds were elucidated by ^{1}H NMR and ^{13}C NMR comparisons with the corresponding compounds in the literature.[26]

3.2. Proposed Biosynthetic Pathways

A possible biosynthetic pathway starting from 2,3-oxidosqualene is shown in Figure 1D. The key intermediate, parkeol, could be synthesized via a chair-boat-chair (C-B-C) conformation prosteryl cation path. Subsequent oxidation of the 21-Me group of parkeol yields dehydrotrametenolic acid, which can undergo a series of hydroxylation and oxidation steps to yield PZI and PZL. 16-Deoxyporicoic acid B is the intermediate product via Baeyer–Villiger oxidation and a 3,4-oxidative cleavage from dehydrotrametenonic acid. Then, a series of protonation, hydroxylation, and esterification steps yield PZJ and PZK.

3.3. Docking Analysis

MMPs have been demonstrated to play a critical role in multi-organ fibrosis. Although MMPs have been considered as therapeutic targets due to their ability to modulate tissue turnover during fibrogenesis, MMP-2, MMP-7, MMP-9, and MMP-13 have been closely associated with kidney injury.[41] The interactions between 11 tetracyclic triterpenoid compounds and MMP-2, MMP-7, MMP-9, and MMP-13 were investigated by docking analysis. Unfortunately, the docking analysis of the compounds and MMP-2 were not performed due to the absence of the crystal structure of MMP-2-ligand in RCSB PDB. Our findings showed that all 11 compounds exhibited different interaction with MMP-7, MMP-9, and MMP-13. Therefore, tetracyclic triterpenoid compounds could be considered MMP inhibitors. To discover specific MMP inhibitors, the docking analysis was performed. The docking results further showed that the four new tetracyclic triterpenoid compounds PZI, PZJ, PZK, and PZL bound to the active sites of MMP-9 and MMP-13 but bound to the non-active sites of MMP-7, implying the selective inhibitory effects of PZI, PZJ, PZK, and PZL on MMP-9 and MMP-13 (**Figure 2**A). Furthermore, PZI, PZJ, PZK, and PZL showed lower free energy requirements and Ki values for interacting with MMP-13 than with MMP-9, indicating the stronger inhibitory effect of PZI, PZJ, PZK, and PZL on MMP-13, rather than MMP-9 (**Table 1**). Moreover, the Ki values of PZI, PZJ, PZK, and PZL were lower than those of the known compounds for interacting with MMP-13. Taken together, the results indicate these four new tetracyclic triterpenoids could be considered specific MMP-13 inhibitors.

Regarding the docking interactions of the four new compounds with MMP-13, all these compounds coordinate with the catalytic Zn^{2+} at the active site of MMP-13 through carboxylic acid function (Figure 2B). Except for PZL, the compounds form a π interaction with His223 at the active site of MMP-13. Moreover, regarding the hydrogen bonding interaction with MMP-13, we found that the carboxylic acid component of PZJ forms a conventional hydrogen bond with Gly184 and the hydroxyl group of PZL forms two hydrogen bonds with Glu224 and Ala187. Apart from the π interaction, PZI can interact with Ile244, Leu185, Leu186, and Val220 via alkyl interactions and with Pro243, Gly184, His188, Glu224, Ala187, Tyr245, and Phe242 via Van der Waals interactions. In addition, PZJ shows Van der Waals interactions with His223, His188, Glu224, Phe242, Tyr215, and Ser183; PZK exhibits Van der Waals interactions with His188, Glu224, Pro243, Ala187, Phe242, and Gly184; and finally, PZL forms Van der Waals interactions with Val220, Tyr245, Tyr215, Ile244, Ser183, Gly184, Pro243, and His233.

3.4. Concentration-Dependent Effects of the Four Poricoic Acids on HK-2 Cells

To assess cell viability and determine the optimal concentration of PZI against MMP-13 and EMT, the effect of different concentrations of PZI on HK-2 cells was determined. The cell viability was 1.00 ± 0.04, 1.05 ± 0.05, 1.03 ± 0.08, 1.07 ± 0.05, and 1.08 ± 0.06 in HK-2 cells exposed to PZI concentrations of 0, 1, 10, 50, and 100 μM, respectively. PZI did not produce a cytotoxic or proliferative effect on HK-2 cells at the above mentioned concentrations. Similar results were observed with PZJ, PZK, and PZL. Therefore, PZI, PZJ, PZK, and PZL were used at 10 μM concentrations in our subsequent experiments to compare the inhibitory effects of these compounds.

3.5. Four Poricoic Acids Attenuated TGFβ1-Induced MMP-7, MMP-9, and MMP-13 Expression in HK-2 Cells

To demonstrate the results of docking analysis, we first examined whether poricoic acids PZI, PZJ, PZK, and PZL could inhibit the expression of MMP-7, -9, and -13 in HK-2 cells, which were induced by TGF-β1. As shown in **Figures 3**A,B, MMP-7, -9, and

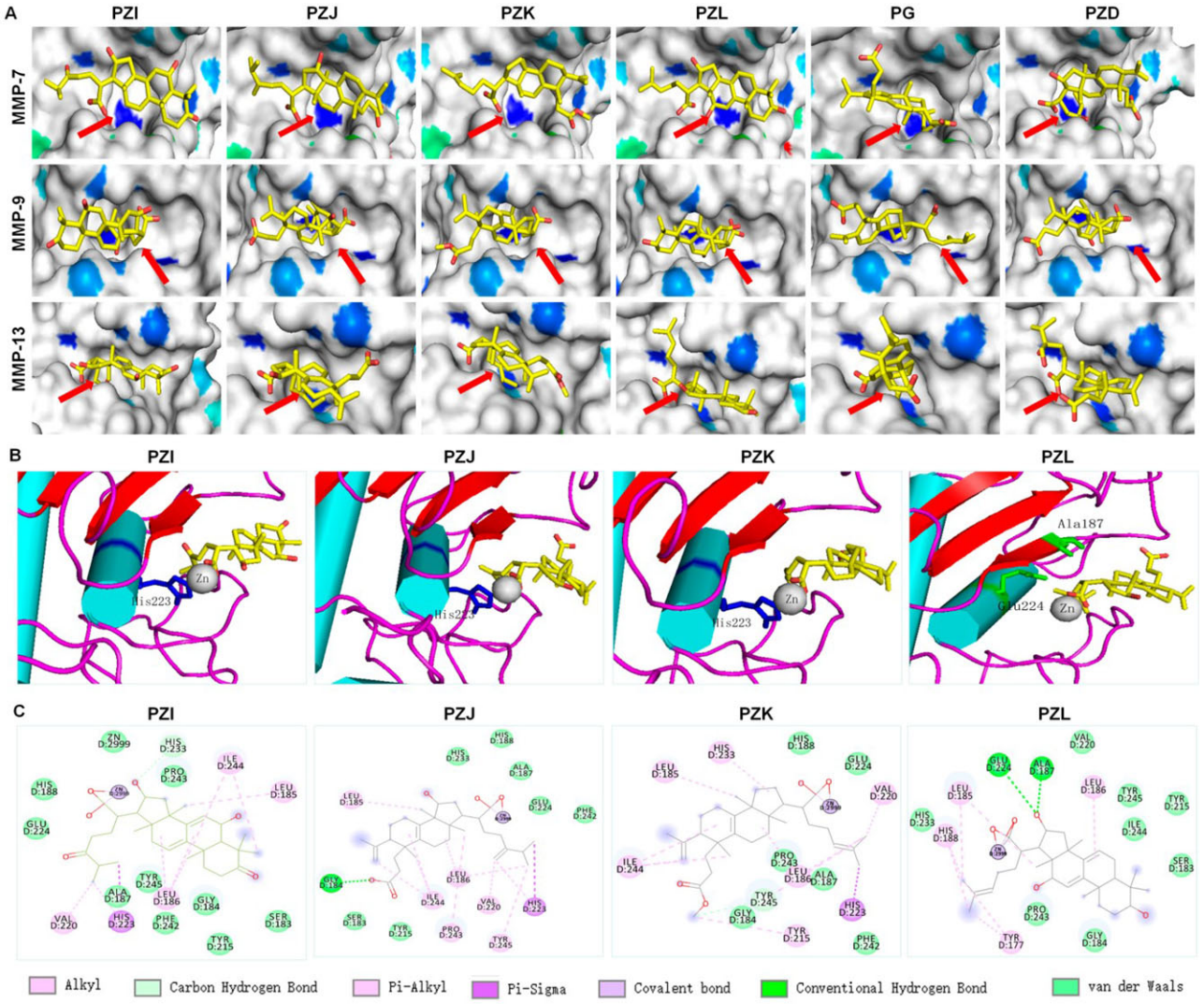

Figure 2. Docking analyses of MMP-7, -9, and -13 and PZI, PZJ, PZK, and PZL. A) Binding models of the compounds in the active sites of MMP-7, -9, and -13. The red arrow indicates the S1' pocket of MMP, and the small molecule is colored yellow. B) Interactions of the compounds with MMP-13. Interacting amino acids are shown in lines, and zinc ions are shown in grey spheres, in which hydrogen bonds are shown in green, π interactions are in blue, and the small molecule is in yellow. C) The docking positions and interactions of the compounds with MMP-13.

Table 1. The binding free energy ($\triangle G$) and inhibition constant (Ki) value of the interactions between compounds and MMPs.

	MMP-7		MMP-9		MMP-13	
	$\triangle G$ [kcal mol^{-1}]	Ki	$\triangle G$ [kcal mol^{-1}]	Ki	$\triangle G$ [kcal mol^{-1}]	Ki
PZI	–	–	−13.96	58.69 pM	−14.46	25.14 pM
PZJ	–	–	−12.26	1.03 nM	−13.51	125.39 pM
PZK	–	–	−12.78	428.96 pM	−13.5	126.81 pM
PZL	–	–	−14.52	22.58 pM	−13.3	176.95 pM
PG	−10.76	13.04 nM	−10	47.02 nM	−12.08	1.39 nM
PZD	−11.44	4.10 nM	−13.49	128.55 pM	−10.25	30.90 nM

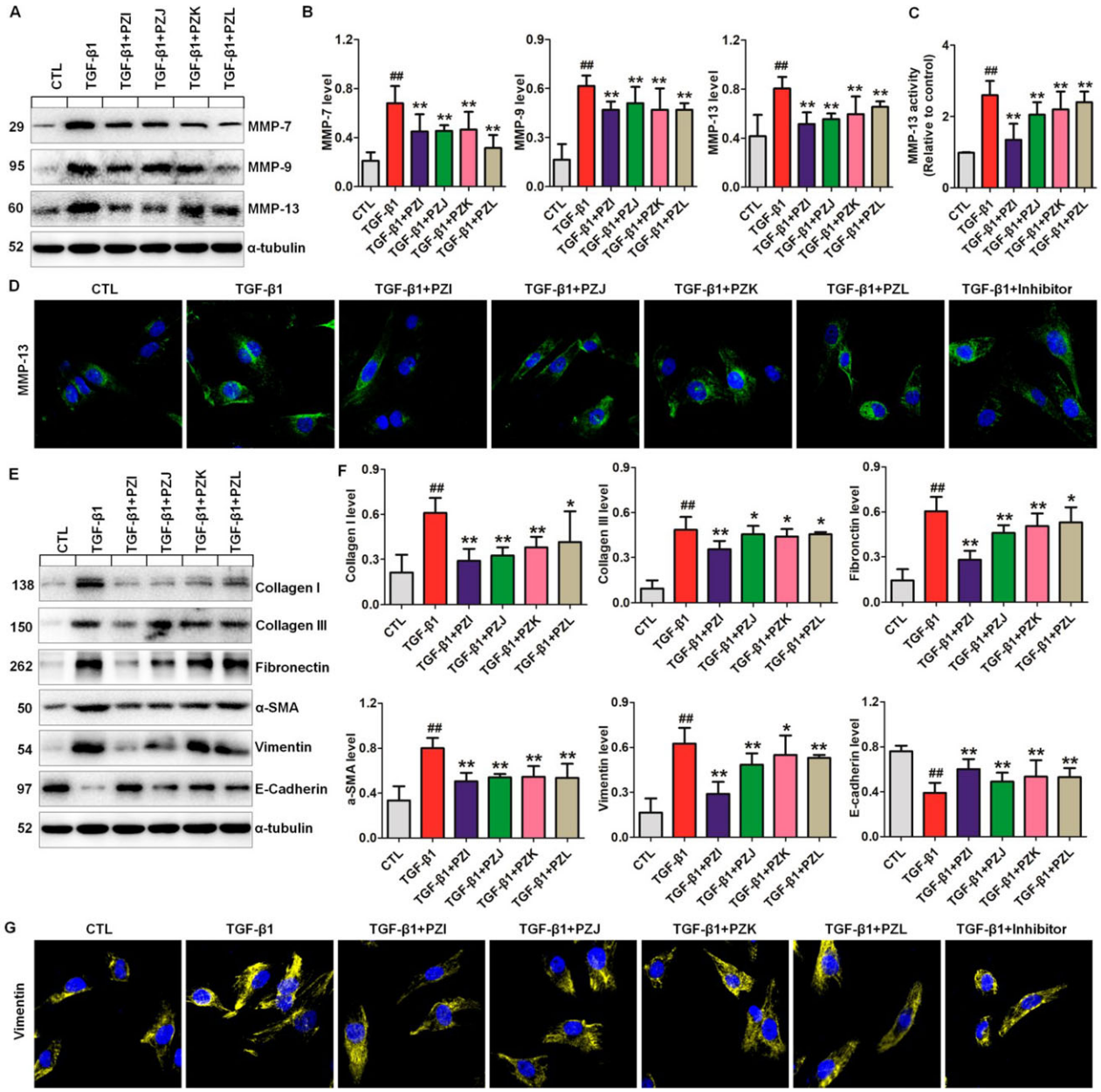

Figure 3. Treatments with PZI, PZJ, PZK, and PZL inhibit MMPs and profibrotic protein expression in TGF-β1-induced HK-2 cells. A,B) Protein expression and quantitative analyses of MMP-7, -9, and -13 in HK-2 cells induced by TGF-β1. C) MMP-13 activity was determined in TGF-β1-induced HK-2 cells treated with PZI, PZJ, PZK, and PZL using a fluorogenic method. D) Representative immunofluorescent staining indicates TGF-β1-induced MMP-13 expression in the different groups. E,F) Protein expression and quantitative analyses of collagen I, collagen III, fibronectin, α-SMA, vimentin, and E-cadherin in HK-2 cells induced by TGF-β1. G) Representative immunofluorescent staining represents TGF-β1-induced vimentin expression in the different groups.$^{\#\#}p < 0.01$ compared with the CTL group; $^{*}p < 0.05$,$^{**}p < 0.01$ compared with the TGF-β1-induced group ($n = 6$).

-13 were significantly increased in TGF-β1-treated HK-2 cells. Treatment with poricoic acids significantly suppressed MMP-7, -9, and -13. Intriguingly, PZL exhibited the strongest inhibitory effects on both MMP-7 and MMP-9 compared with the other three compounds. PZI exhibited the strongest inhibitory effects on MMP-13 of the other three compounds in TGF-β1-induced HK-2 cells. In addition, a significant increase in MMP-13 activity was observed in the TGF-β1-treated HK-2 cells, whereas the rise in MMP-13 activity was partially abrogated by PZI treatment (Figure 3C), events which were in line with our docking results. The inhibitory effect of poricoic acids was confirmed by immunofluorescence staining of MMP-13 protein (Figure 3D).

MMPs make an important contribution to EMT in tissue fibrosis.[20,22,42] We next examined whether PZI, PZJ, PZK, and PZL could inhibit expression of collagen I, collagen III, fibronectin, α-SMA, and vimentin and maintain E-cadherin expression in TGF-β1-induced HK-2 cells (Figure 3E,F). Although all four compounds significantly suppressed expression of

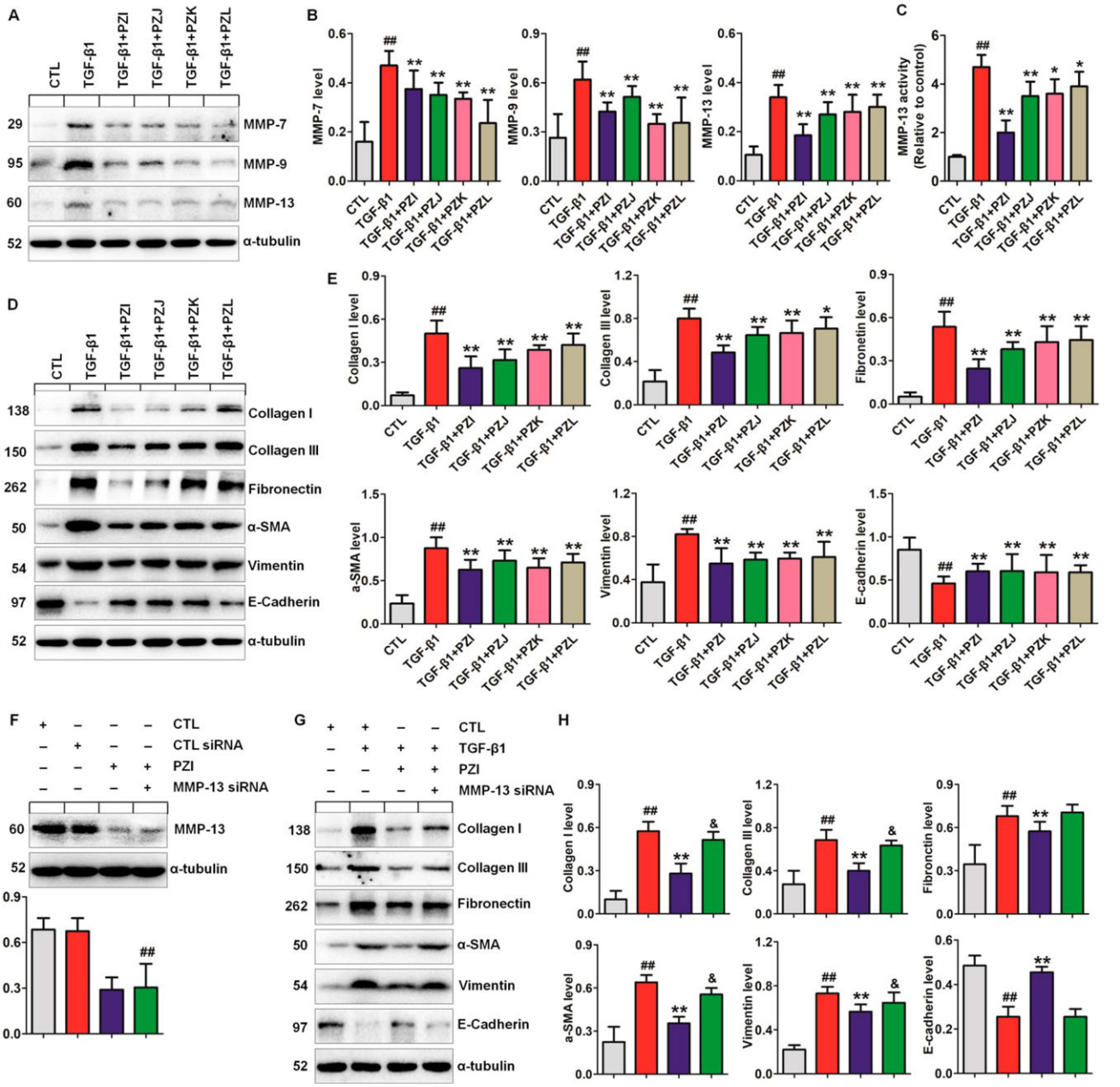

Figure 4. Treatments with PZI, PZJ, PZK, and PZL inhibit MMPs and profibrotic protein expression in TGF-β1-induced NRK-52E cells. A,B) Protein expression and quantitative analyses of MMP-7, -9, and -13 in TGF-β1-induced NRK-52E cells. C) MMP-13 activity was determined in TGF-β1-induced NRK-52E cells treated with PZI, PZJ, PZK, and PZL using a fluorogenic method. D,E) Protein expression and quantitative analyses of collagen I, collagen III, fibronectin, α-SMA, vimentin, and E-cadherin in NRK-52E cells induced by TGF-β1. F) The protein expression of MMP-13 in HK-2 cells induced by MMP-13 siRNA.$^{\#}p < 0.05$,$^{\#\#}p < 0.01$ compared with the CTL siRNA group ($n = 6$). G) After transfection with MMP-13-specific siRNA or scrambled siRNA, protein expression levels of collagen I, collagen III, fibronectin, α-SMA, vimentin, and E-cadherin were determined in TGF-β1-induced HK-2 cells treated with PZI. H) Quantitative analyses of collagen I, collagen III, fibronectin, α-SMA, vimentin, and E-cadherin in TGF-β1-induced HK-2 cells treated with PZI. $^{\#\#}p < 0.01$ compared with the CTL group ($n = 6$); $^{*}p < 0.05$, $^{**}p < 0.01$ compared with the TGF-β1-induced group ($n = 6$); $^{\&}p < 0.05$ compared with the TGF-β1-induced group ($n = 5$ or 6).

EMT-associated proteins, PZI exhibited the strongest inhibitory effects on these proteins compared with the other three compounds (Figure 3E,F). This result was further confirmed by immunofluorescence staining of vimentin protein (Figure 3G). Similar results were observed in TGF-β1-induced NRK-52E (**Figure** 4A–E) and NRK-49F (Figure S1, Supporting Information) cells. EMT led to the transition of epithelial cells (NRK-52E) to interstitial fibroblasts (NRK-49F). Taken together, the inhibitory effect of PZI on EMT and tissue fibrosis was associated with MMP-13 expression.

3.6. PZI Selectively Inhibited MMP-13 and Attenuated EMT in HK-2 Cells

To further determine whether PZI ameliorates EMT by selectively inhibiting MMP-13, HK-2 cells were transfected with control siRNA or MMP-13 siRNA in the absence or presence of PZI. Compared with the control siRNA, MMP-13 protein expression was significantly reduced in HK-2 cells transfected with MMP-13 siRNA (Figure S2A,B, Supporting Information). PZI did not exhibit a significant influence on MMP-13 expression in HK-2 cells transfected with MMP-13 siRNA (Figure 4F). After specific MMP-13 RNAi transfection, EMT-associated protein expression was partially weakened in TGF-β1-induced HK-2 cells (Figure S2C,D, Supporting Information). The inhibitory effect of PZI was also partially weakened, indicating that MMP-13 was one of the most important therapeutic targets of PZI (Figure 4G,H). The inhibitory effect of PZI on MMP-7 and -9 expression was also partially weakened (Figure S3A,B, Supporting Information). Collectively, the results demonstrated that PZI, a novel MMP-13 inhibitor, mitigates EMT by selectively inhibiting TGF-β1-mediated MMP-13 expression.

3.7. PZI Attenuated EMT and Renal Fibrosis by Inhibiting MMPs in UUO Mice

We next examined whether PZI could inhibit MMP-13 and ameliorate renal fibrosis in the kidney tissues of UUO mice. As shown in **Figure 5**A,B, UUO mice exhibited extensive renal fibrosis and significant upregulation of MMP-13 expression. PZI treatment significantly attenuated renal fibrosis and reversed upregulation of MMP-13 activity in UUO mice (Figure 5C), confirming the results of the in vitro experiments. Although PZI treatment significantly attenuated upregulation of MMP-7, -9, and -13 expressions, it exerted stronger inhibitory effects on MMP-13 than MMP-7 and -9 (Figure 5D,E), confirming the results of the in vitro experiments. Furthermore, PZI treatment significantly inhibited the upregulation of collagen I, collagen III, fibronectin, α-SMA, and vimentin and the downregulation of E-cadherin in the kidney tissue of UUO mice (Figure 5D,E). These findings were consistent with the results of the in vitro experiments using HK-2, NRK-52E, and NRK-49F cells.

3.8. PZI Selectively Inhibited MMP-13 and Attenuated EMT in UUO Mice

To confirm the specific effect of PZI on MMP-13, we subjected MMP-13 knockdown mice to UUO. The inhibitory effect of PZI on fibronectin, α-SMA, and vimentin was partially weakened in the MMP-13 knockdown UUO mice (Figure 5F,G). These findings identified MMP-13 as an important therapeutic target of PZI, which serves as an MMP-13 inhibitor.

3.9. Structure-Function Relationship of the New Compounds

Carboxyl, carbonyl, and hydroxyl groups are very important bioactive functional groups of drugs. Our experiments on pharmacological activities and mechanisms of action showed that PZI had stronger bioactivity than the other three new compounds. This result indicated that introduction of carbonyl groups into the carbon atoms at the 3 and 24 positions of the PZI molecule enhanced its antifibrotic effect. In addition, an increasing number of hydroxyl groups of PZI may be associated with its improved bioactivity. Our study suggests that the degree of triterpenoid oxidation is vital for their antifibrotic activity, which is important for understanding the biological activity of antifibrotic triterpenoids.

4. Discussion

Molecular docking is an effective approach for the binding of two or more molecular models based on matching the geometry, chemical structure, environment, and energy in a molecular model. Molecular docking-based discovery of candidate drugs or inhibitors involves matching a library of small molecules to the 3D structure of the targets, such as receptors, enzymes, and ion channels, according to virtual molecular docking techniques. Docking is one of the commonly used approaches that can automatically simulate the ligand's action in the potential active site of the receptor and induce the best mode of interaction. Therefore, molecular docking has been widely used for target structure-based molecular docking screening. In the present study, we employed a combination of a computer-aided virtual approach and small molecule–protein interaction (poricoic acid-MMP) analysis. This approach greatly reduced the number of poricoic acids for actual screening by using in vivo and in vitro models and improved the efficiency of discovering new MMP inhibitors.

An imbalance of MMPs and tissue inhibitors of metalloproteinases (TIMPs) significantly contributes to the pathogenesis of tissue fibrosis.[43,44] MMPs degrade matrix components, including all forms of native collagens, and play a pivotal role in remodelling the extracellular matrix (ECM) in both physiological and pathological conditions. The 24-membered MMP family is highly conserved, with 56–64% sequence similarity in their active domains.[45] MMPs are traditionally classified based on their in vitro ECM substrate specificity into seven main groups including interstitial collagenases, gelatinases, stromelysins, membrane-type MMPs, matrilysins, and metalloelastases, among others.[46] Various disorders can cause fibrosis, which leads to irreversible tissue damage and dysfunction. Since effective therapeutic options to prevent and slow fibrotic changes are limited, establishing effective antifibrotic therapy is urgently needed.

The concept of degrading the ECM to prevent and/or treat tissue fibrosis emanates from the molecular mechanism of fibrosis development. Although some broad-spectrum MMP inhibitors, such as doxycycline, CL-82198, and batimastat, were originally developed as antineoplastic agents, the development of more specific inhibitors may be required for clinical use. Kalm discussed "tawko" or "tawking" as the Indian names for the plant that produce edible roots.[47] Indians use *P. cocos* for making bread,[48] and in Asia, *P. cocos* is usually used to make tea or cake. *P. cocos* has frequently been prescribed as one of the major constituents in compounded prescriptions in natural medicine. Nearly 10% of

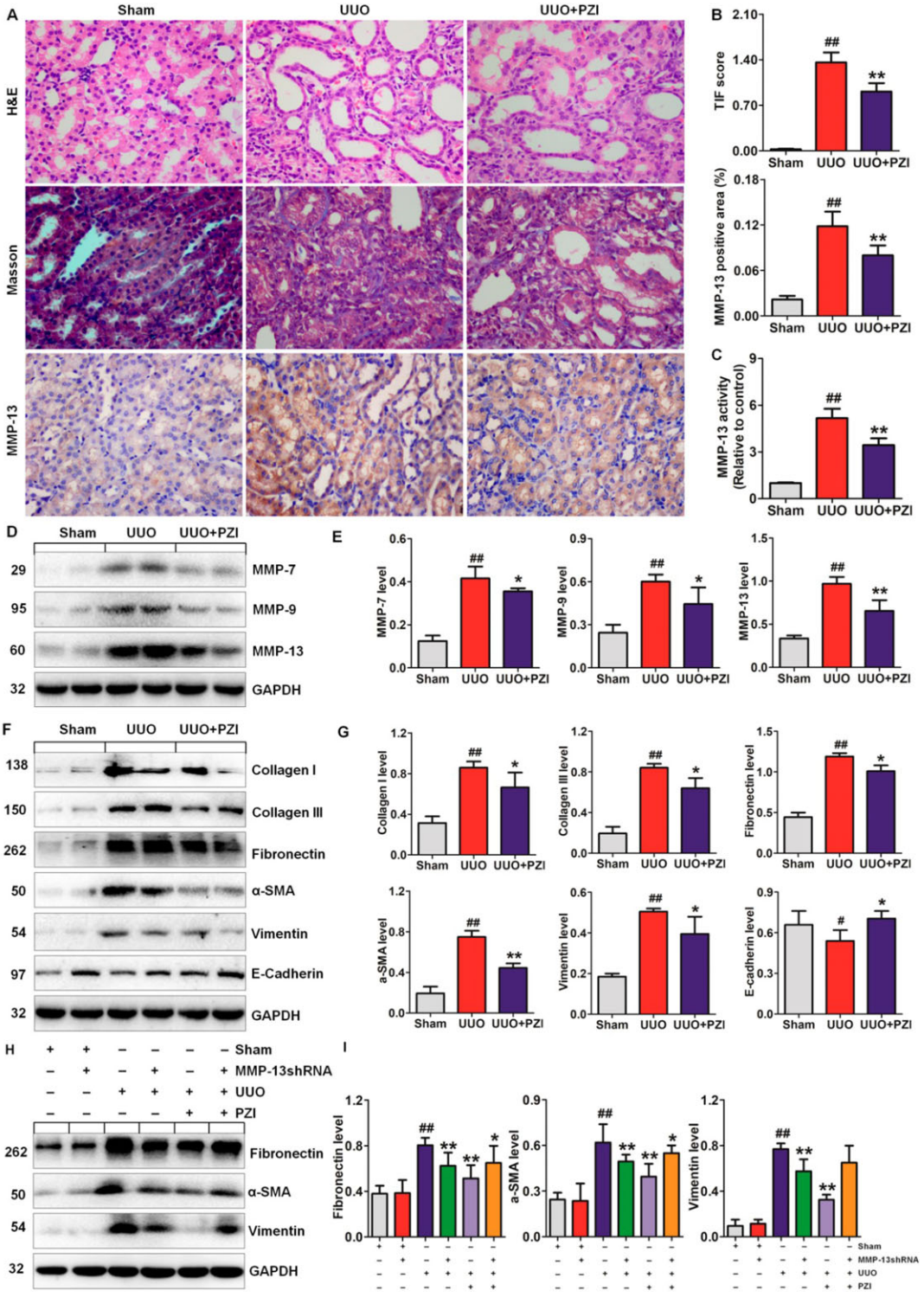

Figure 5. PZI treatment ameliorates renal fibrosis by inhibiting the expressions of MMP-13 and pro-fibrotic proteins in UUO mice. A) Representative micrographs showed kidney injury in the different groups. Paraffin sections were used for H&E, Masson's trichrome, and MMP-13 immunohistochemical stainings. B) Quantitative analyses of Masson's trichrome and MMP-13 immunohistochemical stainings in the different mice. C) The kidney tissues of MMP-13 activity were determined in UUO mice treated by PZI treatment using a fluorogenic method. D,E) Protein expressions and quantitative analyses of MMP-7, -9, and -13 in the different groups of the UUO mice. F,G) Protein expressions and quantitative analyses of collagen I, collagen III, fibronectin, α-SMA, vimentin, and E-cadherin in the different groups of the UUO mice. H) Protein expressions of renal fibronectin, α-SMA, and vimentin of knockdown of MMP-13 in UUO mice by PZI treatment. I) Quantitative analyses of renal fibronectin, α-SMA, and vimentin expression in knockdown of UUO mice as indicated. $^{\#\#}p < 0.01$ compared with sham group. $^{*}p < 0.05$, $^{**}p < 0.01$ compared with UUO group.

the natural medicinal preparations included in the Chinese Pharmacopoeia (2010 edition) contain *P. cocos*.[25] Our recent studies demonstrated that poricoic acids could protect against renal fibrosis by inhibiting renin-angiotensin system activation and regulating TGF-β/Smad and Wnt/β-catenin pathways both in vitro and in vivo.[35,49] Another study demonstrated that dehydroeburicoic acid monoacetate could inhibit cisplatin-induced nephrotoxicity by inhibiting activation (phosphorylation) of the mitogen-activated protein kinases JNK, ERK, and p38 and caspase-3 in renal proximal tubular epithelial cells (LLC-PK1).[50] In the present study, we identified four new tetracyclic triterpenoid compounds (PZI, PZJ, PZK, and PZL) as novel inhibitors of MMPs that downregulated EMT proteins including collagen I, collagen III, fibronectin, α-SMA, and vimentin and upregulated the expression of the antineoplastic agent E-cadherin in TGF-β1-treated HK-2, NRK-52E, and NRK-49F cells. Furthermore, both in vitro and in vivo experiments demonstrated that PZI exerts a strong inhibitory effect on the protein expression and enzyme activity of MMP-13 compared with the other three compounds, which was in line with our docking results. Thus, these data identified PZI as a specific MMP-13 inhibitor and as such, represents a potential therapeutic candidate for limiting EMT and renal fibrosis.

Renal fibrosis progresses via several important phases, including inflammation and oxidative stress, fibroblast/myofibroblast activation, EMT, ECM deposition, and fibrosis.[42,51] EMT plays a critical role in progressive renal fibrosis.[42] EMT is characterized by decreased cell–cell adhesion, upregulated expression of mesenchymal markers such as collagen I, α-SMA, and fibronectin, and downregulated expression of epithelial marker E-cadherin.[42] Mounting evidence has demonstrated the critical role of MMPs in EMT and fibrosis. MMPs have always been regarded as potential therapeutic targets for treating organ fibrosis. MMP-7, -9, and -13 are important members of the MMP family that promote fibrogenesis.

MMP-7 is involved in renal, liver, and lung fibrosis.[39,52] A previous study demonstrated that MMP-7 induced tubular epithelial-interstitial fibroblast communication via the Wnt/β-catenin pathway.[53] Tubular activation of β-catenin following injury mediates EMT and promotes tubular expression and secretion of MMP-7.[54] Upregulation of MMP-7 mediates FasL expression in interstitial fibroblasts. Loss of tubular β-catenin results in enhanced interstitial fibroblast survival due to reduced MMP-7 expression. Consistent with these results, tubular β-catenin loss causes increased interstitial fibroblast survival due to the decline in MMP-7 expression.[53] In fact, experiments using MMP-7 knockout mice demonstrated that MMP-7 mediates activation of β-catenin and promotes renal fibrosis.[53]

Amongst the gelatinases, a number of studies indicate that MMP-9 (gelatinase B) promotes organ fibrosis.[46,55] Under normal condition, MMP-2, MMP-9, and MMP-13 are expressed at low levels in human kidney cells such as mesangial cells and tubular epithelial cells. However, the mRNA expression levels of MMP-2, MMP-9, and MMP-13 are upregulated in renal fibrosis. It has been reported that upregulation of MMP-9 induces EMT and promotes migratory capacity in murine renal tubular epithelial cells.[56] Another study demonstrated that upregulation of MMP-9 mediated EMT in renal tubular epithelial cells via E-cadherin, which led to β-catenin activation.[57] In addition, overexpression of MMP-9 was detrimental by promoting renal interstitial fibrogenesis through a series of processes that led to tubular basement membrane destruction and, in turn, to promotion of EMT.[58] Consistent with these results, deficiency of MMP-9 in mice blocked tubular EMT as detected by α-SMA and attenuated fibrosis in UUO mice.[58]

The major interstitial collagenases that degrade native fibrillar collagens include MMP-1, -8, and -13. MMP-1 is absent in rodents. MMP-8 is expressed predominantly in hematological cells; hence, MMP-13 (also known as collagenase-3) is a major collagenase for ECM resolution, especially related to type I, II, and III collagens in this species.[59] MMP-13 activity can be regulated at multiple levels, including transcriptional regulation, post-transcriptional regulation by microRNAs, epigenetic modification, activation of pro-enzymes, and inhibition by endogenous inhibitors.[60] Increasing evidence suggests that aberrant MMP-13 contributes to cancer, arthritis, atherosclerosis, and fibrosis.[61,62] Compared with the studies of MMP-7 and -9, only a few studies have focused on the investigation of MMP-13 in kidney disease and renal fibrosis. Conde et al. showed that upregulation of MMP-13 expression induced EMT via upregulation of α-SMA and collagen I in rats with renal ischemia/reperfusion.[63] Nakamura et al. reported upregulation of MMP-13 mRNA expression in UUO rats.[64] Sakamaki et al. reported that adriamycin treatment caused a significant increase in renal MMP-13 activity that was accompanied by an increase in MMP-13 mRNA, suggesting that this result could be explained by increased gene transcription, rather than changes in pro-MMP cleavage and/or TIMP expression. The study further showed that deletion of MMP-13 ameliorated glomerular injury compared with the condition in wild-type mice.[65] Expression of mRNA and lncRNA showed MMP-13 expression was significantly increased in renal transplant recipients with urothelial cancer.[66] A previous study demonstrated that MMP-13 exerted collagenase activity through induction of other collagenases, including MMP-2 and MMP-9.[59] MMP-2 is necessary and sufficient for the induction of EMT, and MMP-2 overexpression in transgenic mice promotes renal fibrosis.[67,68] MMPs also mediate the proteolytic shedding of E-cadherin that leads to β-catenin nuclear translocation and Snail2 induction, thus inducing EMT in tubular epithelial cells.[57] Our study indicated that the dysregulation of MMP-13 affected expression of MMP-7 and -9. These findings revealed that MMP interaction promoted renal fibrosis.

5. Conclusions

In summary, docking analysis identified possible binding orientations of poricoic acids on the active sites of MMPs. The study demonstrated the contribution of EMT-13 in the pathogenesis of renal fibrosis and efficacy of PZI, a novel MMP-13 inhibitor, in mitigating EMT and attenuating interstitial fibrosis. Therefore, PZI may be a potential therapeutic candidate for suppressing EMT.

Supporting Information

Supporting Information is available from the Wiley Online Library or from the author.

Acknowledgements

L.C. and G.C. contributed equally to this work. This study was supported by the National Natural Science Foundation of China (Nos. 81872985, 81673578).

Conflict of Interest

The authors declare there is no conflict of interest.

Keywords

chronic kidney disease, epithelial-mesenchymal transition, fibrosis, matrix metalloproteinase, MMP-13, *Poria cocos*, poricoic acid

Received: February 8, 2019
Revised: March 22, 2019
Published online:

[1] M. G. Moloney, *Trends Pharmacol. Sci.* **2016**, *37*, 689.
[2] X. Liu, W. Y. Wu, B. H. Jiang, M. Yang, D. A. Guo, *Trends Pharmacol. Sci.* **2013**, *34*, 620.
[3] H. Hao, X. Zheng, G. Wang, *Trends Pharmacol. Sci.* **2014**, *35*, 168.
[4] X. Gong, N. J. Sucher, *Trends Pharmacol. Sci.* **1999**, *20*, 191.
[5] W. Y. Jiang, *Trends Pharmacol. Sci.* **2005**, *26*, 558.
[6] F. J. Hawkins, D. N. Kotton, *Trends Pharmacol. Sci.* **2018**, *39*, 852.
[7] G. Musso, R. Gambino, M. Cassader, E. Paschetta, A. Sircana, *Trends Pharmacol. Sci.* **2018**, *39*, 387.
[8] L. Chen, T. Yang, D. W. Lu, H. Zhao, Y. L. Feng, H. Chen, D. Q. Chen, N. D. Vaziri, Y. Y. Zhao, *Biomed. Pharmacother.* **2018**, *101*, 670.
[9] H. H. Hu, D. Q. Chen, Y. N. Wang, Y. L. Feng, G. Cao, N. D. Vaziri, Y. Y. Zhao, *Chem.-Biol. Interact.* **2018**, *292*, 76.
[10] R. Loomba, V. Seguritan, W. Li, T. Long, N. Klitgord, A. Bhatt, P. S. Dulai, C. Caussy, R. Bettencourt, S. K. Highlander, M. B. Jones, C. B. Sirlin, B. Schnabl, L. Brinkac, N. Schork, C. H. Chen, D. A. Brenner, W. Biggs, S. Yooseph, J. C. Venter, K. E. Nelson, *Cell Metab.* **2017**, *25*, 1054.
[11] D. Q. Chen, H. Chen, L. Chen, N. D. Vaziri, M. Wang, X. R. Li, Y. Y. Zhao, *Nephrol., Dial., Transplant.* **2017**, *32*, 1154.
[12] D. Q. Chen, G. Cao, H. Chen, D. Liu, W. Su, X. Y. Yu, N. D. Vaziri, X. H. Liu, X. Bai, L. Zhang, Y. Y. Zhao, *Redox Biol.* **2017**, *12*, 505.
[13] Y. Y. Chen, D. Q. Chen, L. Chen, J. R. Liu, N. D. Vaziri, Y. Guo, Y. Y. Zhao, *J. Transl. Med.* **2019**, *17*, 5.
[14] Y. Y. Zhao, H. L. Wang, X. L. Cheng, F. Wei, X. Bai, R. C. Lin, N. D. Vaziri, *Sci. Rep.* **2015**, *5*, 12936.
[15] Y. Y. Zhao, R. C. Lin, *Adv. Clin. Chem.* **2014**, *65*, 69.
[16] Y. Y. Zhao, N. D. Vaziri, R. C. Lin, *Adv. Clin. Chem.* **2015**, *68*, 153.
[17] Y. Y. Zhao, *Clin. Chim. Acta* **2013**, *422*, 59.
[18] H. Zhao, S. X. Ma, Y. Q. Shang, H. Q. Zhang, W. Su, *Clin. Chim. Acta* **2019**, *491*, 59.
[19] Y. Y. Zhao, J. Liu, X. L. Cheng, X. Bai, R. C. Lin, *Clin. Chim. Acta* **2012**, *413*, 642.
[20] D. Q. Chen, Y. L. Feng, G. Cao, Y. Y. Zhao, *Trends Pharmacol. Sci.* **2018**, *39*, 937.
[21] N. Syn, L. Wang, G. Sethi, J. P. Thiery, B. C. Goh, *Trends Pharmacol. Sci.* **2016**, *37*, 606.
[22] X. Qi, L. Zhang, X. Lu, *Trends Pharmacol. Sci.* **2016**, *37*, 246.
[23] F. M. Davis, T. A. Stewart, E. W. Thompson, G. R. Monteith, *Trends Pharmacol. Sci.* **2014**, *35*, 479.
[24] D. Q. Chen, H. H. Hu, Y. N. Wang, Y. L. Feng, G. Cao, Y. Y. Zhao, *Phytomedicine* **2018**, *50*, 50.
[25] Y. Y. Zhao, Y. L. Feng, X. Bai, X. J. Tan, R. C. Lin, Q. Mei, *PLoS One* **2013**, *8*, e59617.
[26] Y. Z. Wang, J. Zhang, Y. L. Zhao, T. Li, T. Shen, J. Q. Li, W. Y. Li, H. G. Liu, *J. Ethnopharmacol.* **2013**, *147*, 265.
[27] H. Miao, Y. H. Zhao, N. D. Vaziri, D. D. Tang, H. Chen, H. Chen, M. Khazaeli, M. Tarbiat-Boldaji, L. Hatami, Y. Y. Zhao, *J. Agric. Food Chem.* **2016**, *64*, 969.
[28] H. Miao, M. H. Li, X. Zhang, S. J. Yuan, C. C. Ho, Y. Y. Zhao, *RSC Adv.* **2015**, *5*, 64208.
[29] D. Q. Chen, Y. L. Feng, L. Chen, J. R. Liu, M. Wang, N. D. Vaziri, Y. Y. Zhao, *Free Radic. Biol. Med.* **2019**, *134*, 484.
[30] Y. Y. Zhao, P. Lei, D. Q. Chen, Y. L. Feng, X. Bai, *J. Pharm. Biomed. Anal.* **2013**, *81–82*, 202.
[31] Y. Y. Zhao, H. T. Li, Y. I. Feng, X. Bai, R. C. Lin, *J. Ethnopharmacol.* **2013**, *148*, 403.
[32] Y. L. Feng, P. Lei, T. Tian, L. Yin, D. Q. Chen, H. Chen, Q. Mei, Y. Y. Zhao, R. C. Lin, *J. Ethnopharmacol.* **2013**, *150*, 1114.
[33] Y. Y. Zhao, X. L. Cheng, F. Wei, X. Bai, R. C. Lin, *Biomarkers* **2012**, *17*, 721.
[34] M. Wang, D. Q. Chen, M. C. Wang, H. Chen, L. Chen, D. Liu, H. Zhao, Y. Y. Zhao, *Phytomedicine* **2017**, *36*, 243.
[35] M. Wang, D. Q. Chen, L. Chen, G. Cao, H. Zhao, D. Liu, N. D. Vaziri, Y. Guo, Y. Y. Zhao, *Br. J. Pharmacol.* **2018**, *175*, 2689.
[36] D. Q. Chen, G. Cao, H. Chen, C. P. Argyopoulos, H. Yu, W. Su, L. Chen, D. C. Samuels, S. Zhuang, G. P. Bayliss, S. Zhao, X. Y. Yu, N. D. Vaziri, M. Wang, D. Liu, J. R. Mao, S. X. Ma, J. R. Zhao, Y. Zhang, Y. Q. Shang, H. Kang, F. Ye, X. H. Cheng, X. R. Li, L. Zhang, M. X. Meng, Y. Guo, Y. Y. Zhao, *Nat. Commun.* **2019**, *10*, 1476.
[37] Z. H. Zhang, F. Wei, N. D. Vaziri, X. L. Cheng, X. Bai, R. C. Lin, Y. Y. Zhao, *Sci. Rep.* **2015**, *5*, 14472.
[38] Z. H. Zhang, N. D. Vaziri, F. Wei, X. L. Cheng, X. Bai, Y. Y. Zhao, *Sci. Rep.* **2016**, *6*, 22151.
[39] H. Chen, T. Yang, M. C. Wang, D. Q. Chen, Y. Yang, Y. Y. Zhao, *Phytomedicine* **2018**, *42*, 207.
[40] J. R. Cole, B. Chai, R. J. Farris, Q. Wang, A. S. Kulam-Syed-Mohideen, D. M. McGarrell, A. M. Bandela, E. Cardenas, G. M. Garrity, J. M. Tiedje, *Nucleic Acids Res.* **2007**, *35*, D169.
[41] R. J. Tan, Y. Liu, *Am. J. Physiol. Renal Physiol.* **2012**, *302*, F1351.
[42] S. Lovisa, M. Zeisberg, R. Kalluri, *Trends Endocrinol. Metab.* **2016**, *27*, 681.
[43] Y. Ma, R. P. Iyer, M. Jung, M. P. Czubryt, M. L. Lindsey, *Trends Pharmacol. Sci.* **2017**, *38*, 448.
[44] Q. Yao, L. Kou, Y. Tu, L. Zhu, *Trends Pharmacol. Sci.* **2018**, *39*, 766.
[45] J. Y. Choi, R. Fuerst, A. M. Knapinska, A. B. Taylor, L. Smith, X. Cao, P. J. Hart, G. B. Fields, W. R. Roush, *J. Med. Chem.* **2017**, *60*, 5816.
[46] V. J. Craig, L. Zhang, J. S. Hagood, C. A. Owen, *Am. J. Respir. Cell Mol. Biol.* **2015**, *53*, 585.
[47] G. F. Weber, *Mycologia* **1929**, *21*, 113.
[48] D. L. Lindner, M. T. Banik, *Mycologia* **2008**, *100*, 417.
[49] L. Chen, D. Q. Chen, M. Wang, D. Liu, H. Chen, F. Dou, N. D. Vaziri, Y. Y. Zhao, *Chem.-Biol. Interact.* **2017**, *273*, 56.
[50] D. Lee, S. Lee, S. H. Shim, H. J. Lee, Y. Choi, T. S. Jang, K. H. Kim, K. S. Kang, *Bioorg. Med. Chem. Lett.* **2017**, *27*, 2881.
[51] S. X. Ma, Y. Q. Shang, H. Q. Zhang, W. Su, *J. Nephrol. Adv.* **2018**, *1*, 4.
[52] M. Roderfeld, *Matrix Biol.* **2018**, *68–69*, 452.
[53] D. Zhou, R. J. Tan, L. Zhou, Y. Li, Y. Liu, *Sci. Rep.* **2013**, *3*, 1878.
[54] Y. Liu, *J. Am. Soc. Nephrol.* **2010**, *21*, 212.
[55] E. Roeb, *Matrix Biol.* **2018**, *68–69*, 463.
[56] T. K. Tan, G. Zheng, T. T. Hsu, Y. Wang, V. W. Lee, X. Tian, Y. Wang, Q. Cao, Y. Wang, D. C. Harris, *Am. J. Pathol.* **2010**, *176*, 1256.
[57] G. Zheng, J. G. Lyons, T. K. Tan, Y. Wang, T. T. Hsu, D. Min, L. Succar, G. K. Rangan, M. Hu, B. R. Henderson, S. I. Alexander, D. C. Harris, *Am. J. Pathol.* **2009**, *175*, 580.

[58] X. Wang, Y. Zhou, R. Tan, M. Xiong, W. He, L. Fang, P. Wen, L. Jiang, J. Yang, *Am. J. Physiol. Renal Physiol.* **2010**, *299*, F973.
[59] H. Abe, K. Kamimura, Y. Kobayashi, M. Ohtsuka, H. Miura, R. Ohashi, T. Yokoo, T. Kanefuji, T. Suda, M. Tsuchida, Y. Aoyagi, G. Zhang, D. Liu, S. Terai, *Mol. Ther. - Nucleic Acids* **2016**, *5*, e276.
[60] K. Yamamoto, H. Okano, W. Miyagawa, R. Visse, Y. Shitomi, S. Santamaria, J. Dudhia, L. Troeberg, D. K. Strickland, S. Hirohata, H. Nagase, *Matrix Biol.* **2016**, *56*, 57.
[61] A. Dufour, C. M. Overall, *Trends Pharmacol. Sci.* **2013**, *34*, 233.
[62] C. H. Ma, C. H. Wu, I. M. Jou, Y. K. Tu, C. H. Hung, P. L. Hsieh, K. L. Tsai, *Redox Biol.* **2018**, *14*, 72.
[63] E. Conde, S. Gimenez-Moyano, L. Martin-Gomez, M. Rodriguez, M. E. Ramos, E. Aguado-Fraile, I. Blanco-Sanchez, A. Saiz, M. L. Garcia-Bermejo, *Sci. Rep.* **2017**, *7*, 41099.
[64] A. Nakamura, A. Ishii, C. Ohata, T. Komurasaki, *Exp. Toxicol. Pathol.* **2007**, *59*, 53.
[65] Y. Sakamaki, H. Sasamura, K. Hayashi, K. Ishiguro, H. Takaishi, Y. Okada, J. M. D'Armiento, T. Saruta, H. Itoh, *Nephron Exp. Nephrol.* **2010**, *115*, e22.
[66] D. Shang, T. Zheng, J. Zhang, Y. Tian, Y. Liu, *Tumor Biol.* **2016**, *37*, 12673.
[67] S. Cheng, D. H. Lovett, *Am. J. Pathol.* **2003**, *162*, 1937.
[68] S. Cheng, A. S. Pollock, R. Mahimkar, J. L. Olson, D. H. Lovett, *FASEB J.* **2006**, *20*, 1898.